



1 **Assessment of the Effect of Soil Amendments and A Three Phase Soil Water Retention Model**

2 ¹Yu Wang*, ¹Yirong Leng, ¹⁻⁶Miklas Scholz, ⁷Nora Hatvani, ¹Vincent Uzomah

- 3 1. School of Science, Engineering & Environment, University of Salford, Manchester UK
- 4 2. aconium GmbH (previously atene KOM), Innovation Management Department, Invalidenstraße
- 5 91, 10115 Berlin, Germany
- 6 3. Department of Civil Engineering Science, School of Civil Engineering, and the Built Environment,
- 7 Faculty of Engineering and the Built Environment, University of Johannesburg, Kingsway
- 8 Campus, PO Box 524, Auckland Park 2006, Johannesburg, South Africa
- 9 4. Kunststoff-Technik Adams, Specialist Company According to Water Law, Schulstraße 7, 26931
- 10 Elsfleth, Germany
- 11 5. Nexus by Sweden, Skepparbacken 5, 722 11 Västerås, Sweden
- 12 6. Department of Town Planning, Engineering Networks and Systems, South Ural State University,
- 13 76, Lenin prospekt, Chelyabinsk 454080, The Russian Federation
- 14 7. Bay Zoltan Nonprofit Ltd, Hungary

15

16 * Corresponding author: y.wang@salford.ac.uk

17

18 **Abstract**

19 Nowadays, using soil amendments to improve physical hydrological properties is popularly employed

20 in agricultural engineering. This paper at first reports an experiment to compare the effect of two

21 different soil amendments for their effect on soil water retention capacity. They two agents are the

22 natural clay and a conditioning soil retainer. Soil water retention curve (SWRC) has been selected to

23 quantify their effect on a benchmark pure sand soil in full range of water saturation, i.e. from fully

24 saturated to nearly dry. Both the classic van Genuchten model and a novel three phase soil water

25 retention model have been adopted to characterize the effect of the two soil amending agents on

26 soil water retention capacity. The research results demonstrate that the clay has a significant

27 enhancement on soil water retention at low content of clay and high soil water content range,

28 however its effect reduces considerable with increasing clay content. Meanwhile the conditioning

29 water retainer shows little effect at high soil water content range but has significant effect on soil

30 water retention at low soil water content range. The results indicate the conditioning water retainer

31 can help the reduction of the surface water evaporation and the water reservation underneath. The



32 modelling has shown that the three-phase model is able to effectively represent the soil water
33 retention curve in full range of soil water content, which provides a convenient tool to efficiently
34 characterise the effect of conditioning water retainer. In addition, the three-phase model also
35 provides the functional analysis and help understand the working mechanisms of the agents.

36

37 **Keywords:** soil amendment; clay; conditioning water retainer; full range soil water retention
38 characteristic modelling.

39

40

1. Introduction

41 Global warming and climate change have caused unstable water supply scenarios worldwide. In
42 Europe, freshwater shortage has been directly impacting on the agricultural industry. Both efficient
43 management for water use and the technologies to improve the water retention capacity of soils
44 have received high interest (Lemos et al., 2021). Nowadays, using soil amendment to improve soil
45 physical hydrological properties is popularly employed in agricultural engineering to enhance the soil
46 water retaining capacity and reduce nutrient loss under challenging environmental conditions
47 (Spitalniak et al., 2019; Xerdiman et al., 2022).

48 There are two types of additive soil amendments in terms of their properties (Seddik et al. 2019).
49 One type comprises natural agents sourced from clay minerals such as attapulgite, bentonite,
50 kaolinite and zeolite (Murray, 2000). The other one is synthetics, such as biochar, superabsorbent
51 polymer (SAP) (Huang et al., 2022), non-woven geotextiles and water absorbing geo-composites
52 (Orzeszyna et al., 2006; Mohawesh and Durner, 2019). Both types can effectively improve soil water
53 retention to reduce both water infiltration below the surface and evaporation at the surface
54 (Keiblinger and Kral, 2018; Spitalniak et al., 2021).

55 In general, the soil water retention capacity basically depends upon the soil texture and pore
56 structure. The underlying physical mechanisms are based on the interfacial molecular interaction
57 forces at the soil particle surfaces and the derived condensing action due to capillarity (Dontsova et
58 al., 2004; Zhang and Lu, 2020). The conventional assessment of the soil water retention capacity takes
59 an approach using the soil water retention curve (SWRC), an intrinsic soil constitutive relation
60 between the soil water content and soil matric suction. SWRC also plays a key role in the prediction



61 for the soil hydraulic conductivity and diffusivity on the concept of their intrinsic link with soil pore
62 size distribution and particle size. For this reason, soil water retention curve has also been widely
63 employed to assess the influence of soil amendments on soil water retention improvement
64 (Spitalniak et al., 2019; 2021; Wanniarachchi et al., 2019; Miller et al., 2018; Edeh & Mašek, 2022;
65 Huang et al., 2022; Zhou et al., 2020; Wang et al., 2023).

66 Modelling SWRC has been a longstanding research topic (Chang and Cheng 2018; de Rooij et al 2021;
67 de Rooij 2022). So far, numerous mathematical models have been proposed in different formulation
68 by different approaches (Du, 2020). Among them, the mathematical formula proposed by van
69 Genuchten (1980) is still the most popular one, which has been widely used in both hydrology and
70 geotechnics, as it provides an effectively convenient way for the hydraulic conductivity prediction.
71 There were many revisions ever proposed on the original van Genuchten's formula (Lima and Silva,
72 2022; Huang et al., 2022). In recent decades, great efforts have been made to interpret the water
73 retention curve from both capillarity and surface adsorption to improve the modelling of soil
74 hydrological properties, particularly from very low water content states to fully saturated state. They
75 include the segmental modelling (Du, 2020; Wang et al., 2022), which divide the water retention
76 curve into two different parts for the adsorption and capillarity, respectively, and a combined
77 sorption-isotherm and capillary model (Wang et al., 2022). However, the segmental modelling may
78 be inefficient to accurately reflect the fact that the surface adsorption and capillary condensation are
79 coexisting at all unsaturated ranges. On the other hand, the formulas of the combined sorption-
80 isotherm and capillary model presents a complex procedure when used for modelling
81 characterization.

82 On the concept of capillarity, soil matric suction is attributed to the interfacial meniscus formed
83 between the air and the bulk water in pore spaces, and the Laplace's equation is employed to
84 evaluate the suction by soil pore size distribution (Dullien, 1991). On the fact that the bulk water in
85 unsaturated soils starts to accumulate from the angular corner spaces of all pores regardless of size,
86 Tuller et al. (1999) tried to address the water sorption and capillary contribution to metric suction
87 within one framework. They proposed to explicitly define the soil matric suction using an augmented
88 Young-Laplace equation consisting of two components. One is to represent the capillary pressure
89 related to the meniscus formed at the interface of the bulk water in pores, which is evaluated by the
90 Laplace's equation. The other one is to represent the surface adsorption force related to the water
91 film on surfaces of empty pores. The effect of the surface adsorption force is evaluated by the water



92 film thickness in terms of the concept of disjoining pressure (Iwamatsu and Horii 1996). Meanwhile
93 a series of pore geometric model were proposed to represent the soil pore network at microscopic
94 scale (Tuller et al. 1999). Following the work by Tuller et al. (1999), such pore-scale modelling for
95 water retention curves (WRC) using the disjoining pressure to estimate the water film effect has also
96 been reported by other researchers, but using different pore geometric models (Or and Tuller, 1999;
97 Likos, 2009; Lebeau and Konrad, 2010; Tokunaga, 2011; Mohammadi and Meskini-Vishkaee, 2012;
98 Beckett and Augarde, 2013).

99 Although these efforts before have demonstrated that the water film on the surface of empty pores
100 at unsaturated states makes a significant contribution to the matric suction, there are still challenges
101 and ineffectiveness faced by these evaluating approaches. Firstly, to rigorously calculate the
102 adsorptive suction component requires a deterministic relationship between the water film thickness
103 and the pore water content and vice versa. However, most of these pore-scale modelling for WRC
104 simply used a mean-field model of the capillary condensation in a slit-type pore (Iwamatsu and Horii,
105 1996) to estimate the effect of the wetting film. Secondly, it is difficult to take account of the water
106 film configuration on soil particles, because it varies with the thickness and the convex curvature of
107 particles. The latter one theoretically consists of a negative contribution to matric suction (decrease
108 of the matric suction). Thirdly, the pore-scale modelling generally simplifies the complexity of the
109 realistic pore geometric shape. At last, the suction worked out at pore-scale does not equal to that
110 at macroscopic bulk soil scale. The latter one is a volume average of all the values at individual pores.
111 To simplify the geometric pore structure modelling, Wang et al. (2008) ever proposed a physical-
112 chemical model for SWRC, which also starts from the concept that surface water film and condensed
113 bulk pore water coexist in unsaturated pore network (Wang et al., 2012), but the soil matric suction
114 is evaluated by volume average theorem.

115 This paper at first reports an experimental test measuring the influence of two types of soil amending
116 agents, i.e. natural clay and a conditioning water retainer, on the SWRC. The control soil (benchmark)
117 is pure sand, which was amended using different percentage of clay and different concentration of
118 the conditioning water retainer. Drying soil water retention curves (SWRCs) were measured using the
119 evaporation method starting from fully saturated up to nearly dry. The full range SWRCs were
120 measured using two different approaches. One is using the HYPROP device to directly measure the
121 SWRCs at low suction range or high water content range. The other one is using environmental
122 chamber to control the relative humidity for the SWRCs at high suction range or low water content



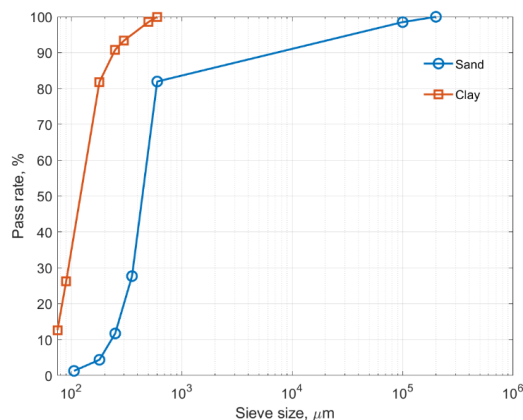
123 range. Thereafter, a new three-phase SWRC model were adopted to represent the measured SWRCs
124 and compared with the van Genuchten modelling. Finally, the three-phase model has been employed
125 to characterize the effect of the WR usage on SWRC.

126

127

2. Materials and Experiment

128 The control/benchmark soil is a pure sand with particle sizes in the range from 0.06 mm to 2 mm.
129 One of the soil amendments is a pure clay with the maximum particle size about 500 μm . Fig. 1 shows
130 the particle size distribution of the sand and clay. The other soil amendment is a conditioning water
131 retainer (WR) developed by the Water & Soil[®] Ltd in Hungary. Unlike conventional soil amendments,
132 such as biochar as well as mineral or polymer gel additives, which in general stand as an independent
133 solid phase mixed into the soil particles, the WR agent here is in liquid form, which is diluted using
134 water before applied on soils.



135

136 Fig. 1. Particle size distribution of the used sand and clay

137

138 The state-of-the-art equipment, HYPROP-2 (Meter Group), was used to measure the drying SWRCs
139 curves at low suction range or high soil water content range within its measuring capacity. The
140 corresponding part of the SWRCs in the range of high suction or low soil water content were
141 measured indirectly by relative humidity equilibrium approach using an environmental chamber to
142 control the relative humidity stepwise. The two measuring approaches cover a wide SWRC range



143 starting from fully saturated state up to nearly dry. Table 1 lists out the prepared soil samples with
144 and without soil amendments.

145

146 Table 1. The Soil samples for the SWRCs test

Samples	Components		
	Sand (% by weight)	Clay (% by weight)	Water retainer (% by volume of water)
Sand (Control)	100	0	1,2,3,5
Clayey sand A	70	30	1,2,3,5
Clayey sand B	50	50	1,2,3,5

147

148 Both sand and clay were dried separately at first in an electrical oven at 110°C for 24 hours to achieve
149 100% dryness before made the samples. Meanwhile, the WR was added to the distilled water to
150 prepare the solutions of four WR concentrations by weight (1%, 2%, 3% and 5%).

151 **2.1. Measuring SWRCs at the range of low suction or high soil water content**

152 The tests were performed using HYPROP-2. A certain weight of the oven dried soils were taken,
153 measured and loaded into the sample ring of HYPROP-2. The amount of the soils just reaches the full
154 volume capacity of the rings given slightly compacting. Thereafter, the soil-loaded HYPROP-2 sample
155 rings were put into glass containers filled with either distilled water or the WR water solution of the
156 defined volume percentages in the Table 1. The surface of the water within the container was kept
157 at 2/3 of the height of the sample rings. The pressure sensors and the base unit of the HYPROP-2
158 were degassed and set-up following the procedure outlined in the operation menu. After 24 hours,
159 all soil samples bathed in the containers, assumed been fully saturated, were taken out and installed
160 on the set-up HYPROP-2 unit to start the tests. All the tests thereafter were conducted automatically
161 until the HYPROP-2 run out of its measurement range/capacity.

162 **2.2. Measuring SWRCs at the range of high suction and low soil water content**

163 The tests were performed using an environmental chamber. Distilled water or the WR water solution
164 of the volume percentages in the Table 1 was little by little added into the oven dried soils until soils
165 became fully saturated. Thereafter, they were loaded into aluminium containers of the dimensions:



166 54 mm in diameter and 30 mm in height. The saturated soil samples in the containers were further
167 compacted using a stoper at the top to reach a height of 20 mm within the containers. Thereafter,
168 all the prepared soil samples were weighed again and then put into the environmental chamber. The
169 environmental chamber was set for a series of controlled relative humidity (RH) magnitudes, which
170 were 90%, 75%, 60%, 45%, 30%, 20% and 10%, by stepwise. The soil samples were left under a certain
171 RH magnitude for an enough long period of time. In the time, the soil water content was monitored
172 by weighting on a scale with an accuracy of 0.01 g until the samples reached a stable state with no
173 weight change detected for at least 1 week, when the soil pore water was assumed have reached an
174 equilibrium state, before RH was set further down one step.

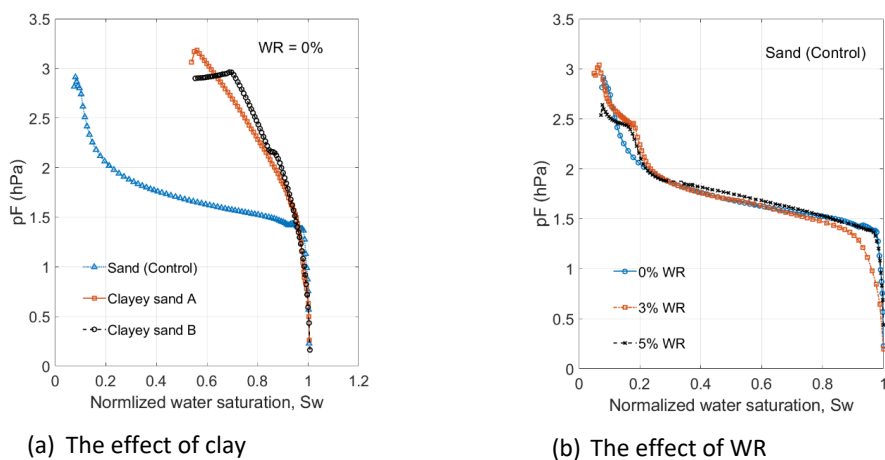
175

176

3. Results and Discussion

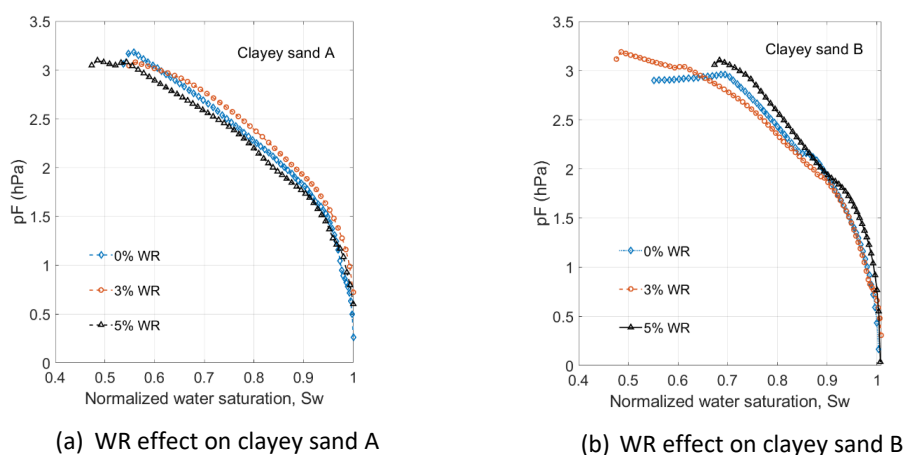
177 Fig. 2 shows the SWRC measurements of the HYPRO-2 tests. It can be seen that the clay amendment
178 has significant effect on the water retention capacity enhancement for the control sand soil. The 30%
179 clay content by weight has an average water saturation increase by about 3 times at a certain suction
180 value in the range of $pF = 2 \sim 3$ (or suction = 100 ~ 1000hPa). However, when the clay content is over
181 30% the effect on soil water content increment becomes much less. The effect of the clay on water
182 retention improvement is more pronounced at relatively low soil water content or high suction value.
183 A logical explanation for the observation is that the clay particles increase the total pore surface area
184 of soil samples and reduces the average pore size, which enhances the relative amount of water film
185 absorbed on pore surfaces and the condensed bulk water in pore volume. This also explains why the
186 effect is more pronounced at high suction end. On the other hand, the total pore surface area
187 increase is not in a linear trend with the increase of clay content. Compared with the clay, the WR
188 amendment has displaced little effect on water retention enhancement in the suction range, $pF = 0$
189 ~ 3, or the corresponding water saturation range, $S_w = 0.2 \sim 1$. Fig. 3 compares the effect on the
190 SWRCs when WR was used for the clay amended soils. Compared with the sand soil, the WR shows
191 increased effect helping water retention at the tested WR concentrations up to 5%, particularly for
192 the clayey sand B.

193



194

Fig 2. The effect of the two amendments on SWRC at low suction range



195

Fig. 3. The WR effect on SWRCs of clayey sands at low suction range

196

197 The measurements in Figs.2 and 3 show that for sand, the HYPROP-2 can only reach the maximum
198 suction $pF = 3$ or the lowest water saturation $S_w = 0.1$. However, for the two clayey sands, the lowest
199 water saturation can only reach at about $S_w = 0.5$, i.e. half saturated. For the part of the SWRCs at
200 lower water content, the tests using the approach of relative humidity control and an environmental
201 chamber were performed. The measurements of the environment chamber tests are given out in
202 Figs. 4 and 5. The SWRCs are in the form of the relative humidity (RH) versus soil pore water



203 saturation. For the RH control tests, the capillary pressure or suction can be evaluated in terms of the
 204 Kelvin equation (Eq. (1)) according to Fredlund (1989).

205

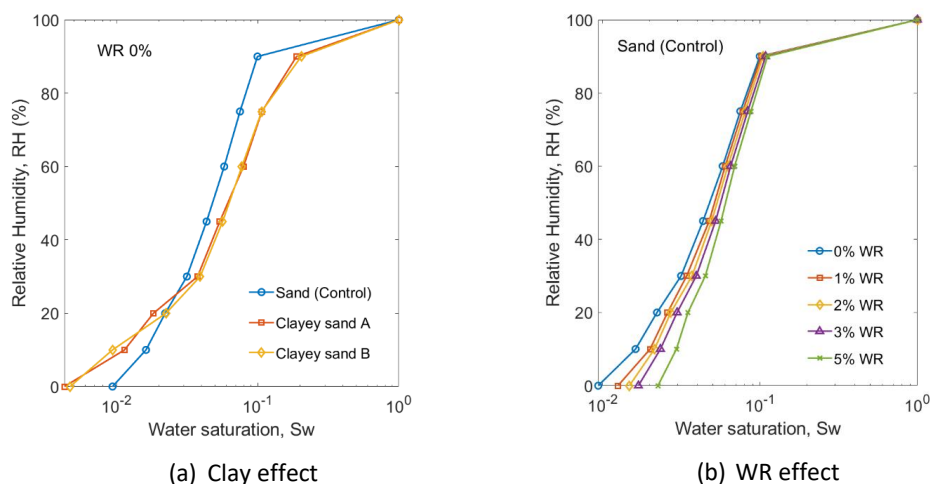
$$206 \quad \psi_m = -RT \ln(RH) / V_w \quad (1)$$

207

208 where ψ_m is the matric suction (Pa) with a positive value, R is the gas constant (8.314 J/mol), T is
 209 Kelvin temperature (set as room temperature at 21°C), RH is the relative humidity and V_w is the water
 210 molar volume, which is about $18.03 \times 10^{-6} \text{ m}^3/\text{mol}$ at room temperature.

211 Fig. 4(a) shows that the 30% clay amendment has the noticed effect on soil water content increase
 212 at a certain controlled RH when $RH > 25\%$. However over 30% clay amendment, the effect almost
 213 unnoticeable. The result is in consistence with that observed in Fig. 2(a). When $RH < 25\%$, the water
 214 retention capacity becomes worse for the clayey sands, compared to the control sand soil. This could
 215 be explained by that there is remaining pore water in clayey sands at such low water level because
 216 of the increase of inaccessible pores at that water content range.

217



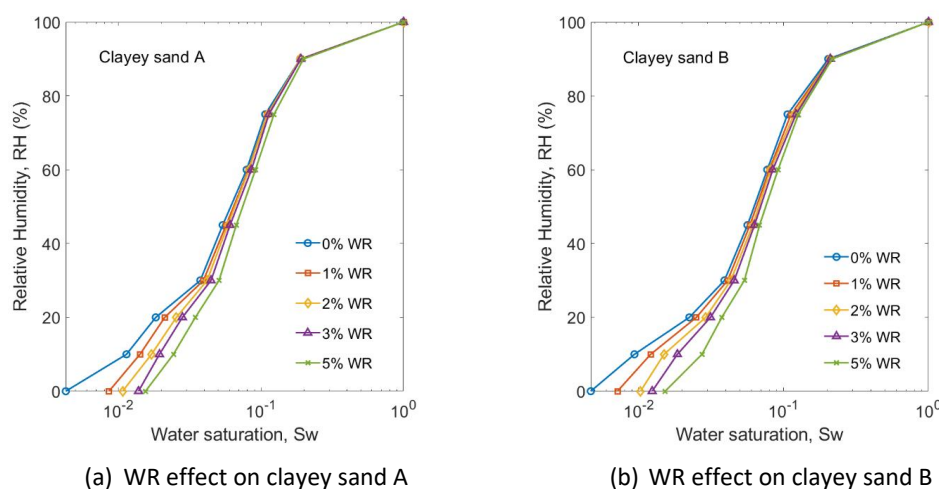
218 Fig. 4. The influence of two soil amendments on the sand soil retention curves controlled by RH
 219 magnitude

220



221 Fig. 5 compares the effect of WR amendment on the SWRCs of the clayey sand soils. Contrast to the
222 results in Fig. 3 for the part at high water content range, it can be seen that the WR amendment
223 displaced noticeable effect enhancing the soil water retention capacity at low water content range.
224 The lower the soil content, the higher the enhancing effect of the WR amendment. Meanwhile, the
225 enhancing effect increases with the WR concentration. The results indicate the WR helps enhance
226 the amount of water in the form of the film on pore surfaces. In the other word, the WR agent
227 particularly increases the surface force between the soil particles and the pore water film. The
228 comparison of the Fig. 5(a) and (b) further shows that the WR effect is quite similar on both clayey
229 sands. This reflects the previous reasoning that the total pore surface area increase is not in a linear
230 trend with the increase of clay content.

231



232 Fig. 5. The effect of the water retainer (WR) on the SWRCs of clayey sands at low water content

233

234

4. Soil Water Retention Characteristic Modelling

235 To quantify the effect of soil amendment on the SWRCs, two models were compared in this study.

236 One model is based on the van Genuchten formula (1980) in the form of the Eq. (2).

237



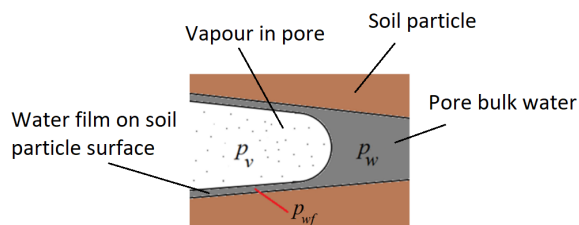
$$238 \quad S_e = \left[\frac{1}{1 + (\alpha \psi_m)^n} \right]^{(1 - \frac{1}{n})} \quad (2a),$$

$$239 \quad S_w = S_r + (S_s - S_r) \left[\frac{1}{1 + (\alpha \psi_m)^n} \right]^{(1 - \frac{1}{n})} \quad (2b),$$

240

241 where $S_e = \frac{S_w - S_r}{S_s - S_r}$ is the effective soil water saturation degree, S_w is the water saturation, S_r is the
 242 residual water saturation, S_s is the fully saturated water saturation; ψ_m is the matric suction (Pa); and
 243 α (1/Pa) and n are two parametric constants.

244



245

246 Fig. 6. The water at pore scale in unsaturated soils

247 p_v - pore vapour pressure; p_w - bulk pore water pressure; p_{wf} - pore water film pressure

248

249 The other one is a new three phase model, a revision on an ever-proposed physicochemical model
 250 for static water retention in unsaturated porous media (Wang et al., 2008; Wang, 2010; Wang et al.,
 251 2012). As illustrated in Fig. 6, for unsaturated soils, three water phases coexist in pore space, they
 252 are the bulk water phase in the filled pore volume; the water vapour in the empty pore volume; the
 253 water film on the empty pore surfaces. In terms of the pressure of mixtures, the pore water matric
 254 potential is determined by the state of the three phases together, which therefore can be expressed
 255 in the form of the Eq. (3) below.

256

$$257 \quad \psi_m = P_c + P_s = (\langle p_w \rangle - \langle p_b \rangle) + \langle p_{wf} \rangle \quad (3)$$



258

259 where, $P_c = (\langle p_w \rangle - \langle p_b \rangle)$ is the capillary pressure evaluated by the interfacial meniscus between
 260 bulk pore water and the pore vapour; $P_s = \langle p_{wf} \rangle$ is the average pressure of the entire water film on
 261 empty pore surfaces, i.e., surfaces of soil particles. The bracket, $\langle \rangle = \frac{1}{V_{REV}} \int_0^{V_{pore}} dV$, is an operator
 262 for the volume average of bulk soil. The V_{REV} stands for representative elementary volume of soil,
 263 and V_{pore} is the total pore volume in the V_{REV} . The pore-scale pressure of the three phases can be
 264 evaluated by the Kelvin equation, Eq. (4), below.

265

$$266 \quad p_{fi} = p_0 \exp\left(\frac{\overline{\Delta\mu_{fi}}}{RT}\right) \quad (4)$$

267

268 where p_{fi} is the average gauge pressure of the fluid phase i on an adsorption surface (i.e. soil particle
 269 surfaces); $\overline{\Delta\mu_{fi}}$ is a local average intrinsic molar chemical potential change of the fluid phase i and it
 270 is defined as $\overline{\Delta\mu_{fi}} = \frac{1}{h} \int_0^h \Delta\mu_{fi}(z) dz$, where h is the thickness fluid phase on the adsorptive substrate
 271 surface, and $\Delta\mu_{fi}(z)$ is the molar molecule potential change of the fluid phase at position z above
 272 the substrate surface. R is the gas constant; T is the temperature; p_0 is a normal pressure.

273 According to the understanding, the volume average pressure for the bulk water phase can be
 274 worked out as: $\langle p_w \rangle = \frac{1}{V_{REV}} \int_0^{S_w V_{pore}} p_w dV$, where S_w is the pore water saturation degree. Similarly,
 275 the volume average pressure for the coexisting bulk vapour phase can worked out to be: $\langle p_v \rangle =$
 276 $\frac{1}{V_{REV}} \int_0^{(1-S_w)V_{pore}} p_v dV$. Substituting Eq. (4) into the integration for the volume average of pressure,
 277 the volume average of the capillary pressure can be determined as shown in Eq. (5) (Wang et al.,
 278 2012).

279

$$280 \quad P_c = \lambda \left[\frac{1}{\alpha} (\exp(\alpha S_w) - 1) - \frac{1}{\beta} (\exp(\beta(1 - S_w)) - 1) \right] \quad (5)$$

281

282 where λ is a constant relevant to the porosity (V_{pore}/V_{REV}) and the initial water film condition when
 283 bulk water starts to accumulate in pore volume due to capillary condensation; α is a constant relevant



284 to the interfacial force between the condensed water phase and the soil particles, while θ is a
285 constant relevant to the interfacial force between the vapour phase and the pore wall surfaces.

286 To evaluate the water film component $\langle p_{wf} \rangle$ in Eq. (3), a t-curve model was adopted here. t-curve is
287 a plot of the statistical thickness of the adsorbate liquid film on the surface of nonporous adsorbents
288 at varied adsorbate vapour pressures. It plays an important role in pore structure analysis and
289 provides an alternative method to estimate the specific surface area of porous media in addition to
290 the BET model (Mikhail et al., 1968; Monnier et al., 2010). De Boer et al. (1966) reviewed three
291 empirical models which had been successfully used to represent the measurements of the nitrogen
292 adsorption isotherms of nonporous adsorbents, which are the modified BET model (Eq. 6(a)), the
293 Harkins-Jura model (Eq. 6(b)) and the Frenkel-Halsey-Hill model (Eq. 7(c)). The three models have
294 become useful tools in pore structure analysis (Christos et al., 2004; Soboleva et al., 2010).

295

$$296 \quad t = \frac{V}{V_m} = \frac{ck(p/p_0)}{(1-k(p/p_0))(1+(c-1)k(p/p_0))} \quad (6a)$$

$$297 \quad \log(p/p_0) = B - \frac{A}{t^2} \quad (6b)$$

$$298 \quad p/p_0 = \exp\left(\frac{-C}{t^r}\right) \quad (6c)$$

299

300 where t is the statistic water film thickness and p/p_0 is the vapour relative pressure, which decides
301 the intrinsic potential of the water film at the thickness t and can be described using the Kelvin
302 equation (Eq. (4)). Comparing Eq. (4) with Eq. (6c), we may obtain Eq. (7).

303

$$304 \quad \frac{\overline{\Delta\mu_{wf}}}{RT} = \frac{-C}{t^r} \quad (7)$$

305

306 In unsaturated soils, the $\overline{\Delta\mu_{wf}}$ decides the pressure of the water film on empty pore wall surfaces
307 and t is linked to the pore water saturation degree. Based on this concept, a power function (Eq. (8))
308 is suggested here to describe the contribution of the water film to the matric suction in terms of pore
309 water saturation.



310

$$\langle p_{wf} \rangle = \chi(1 - S_w)^n \quad (8)$$

312

313 where c and n are two constants; and S_w is the pore water saturation degree.

314 Substituting Eq. (5) and (8) into the Eq. (3), the matric potential (or suction) of unsaturated soils can
315 be expressed in the form of the Eq. (9).

316

$$\psi_m = \lambda \left[\frac{1}{\alpha} (\exp(\alpha S_w) - 1) - \frac{1}{\beta} (\exp(\beta(1 - S_w)) - 1) \right] + \chi(1 - S_w)^n \quad (9)$$

318

319 In the next section, Eqs. (2) and (9) are used to represent the SWRCs measured in the preceding
320 experimental tests.

321

5. SWRCs Modelling

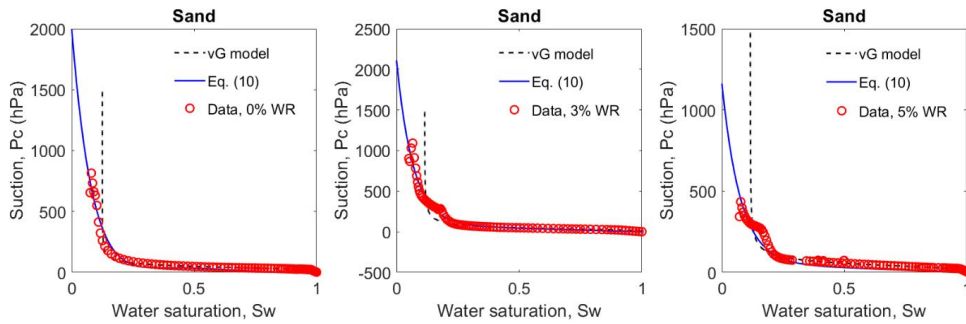
322

5.1. Soil water retention curves at the low suction range

323

324 Fig. 7 compares the modelling results using the van Genuchten model (Eq. (2)) and the three-phase
325 model (Eq. (9)) to represent the SWRC measurements of the HYPROP-2 tests. The results
326 demonstrate that both characteristic models present a good representation for the SWRC at low
327 suction (or high-water saturation) range for all three soils at three different levels of WR application.
328 However, when suction increases (or water saturation reduces) below a certain value, the van
329 Genuchten (vG) model diverts away from the trend of the experimental data but the three-phase
330 model keeps a good fit to the measurements.

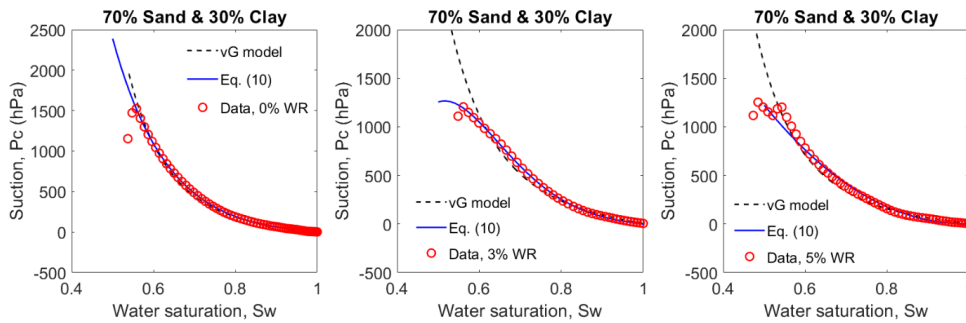
331



3

333

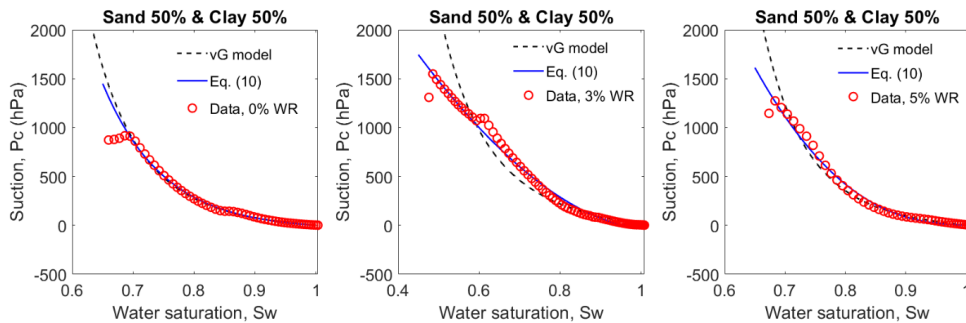
(a) Sand (Control) with three different WR applications



3

335

(b) Clayey sand A with three different WR applications



3

337

(c) Clayey sand B with three different WR applications

338

Fig. 7. Modelling of the SWRCs measured by HYPROP-2 tests

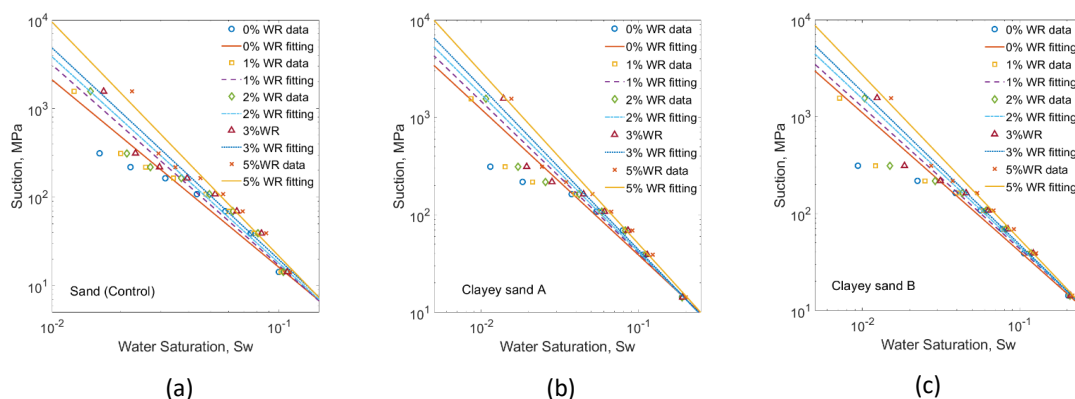
339

340 **5.2. Soil water retention curves at the high suction range**



341 Figs. 8 and 9 compares the results using the Eqs. (2) and (9), respectively, to represent the SWRC
342 measurements of the environmental chamber tests. Fig. 8 shows that the van Genuchten (vG) model is
343 ineffectively representing both the SWRCs of all the three soils and the effect of the WR at varied
344 application levels on the SWRC. For all measurements, Eq. (2) diverts away from the SWRC trend when
345 the suction is higher than 124 MPa (or the controlling RH is lower than 40%). The fitting curves indicate
346 that WR effect on water retention is particularly active at low water content and increases with the
347 concentration.

348



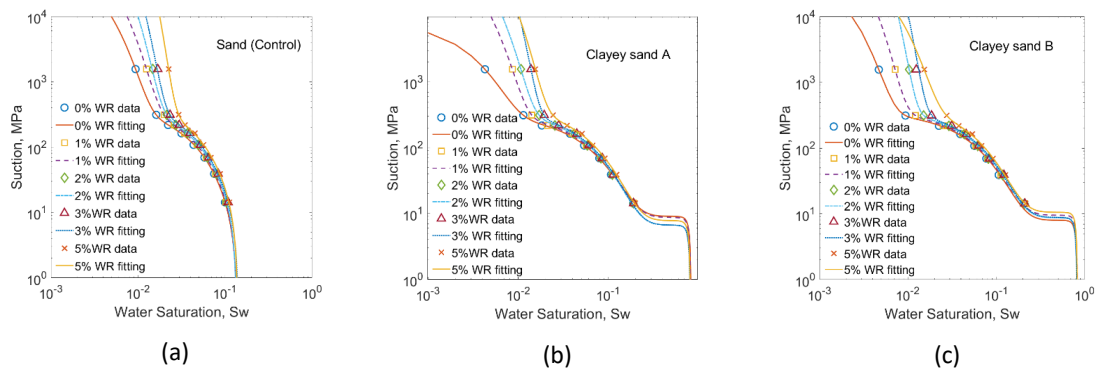
349 Fig. 8. The vG model modelling of the SWRCs measured by relative humidity control tests

350

351 Fig. 9 shows that the proposed three-phase model has well represented all the SWRCs measured by
352 the relative humidity (RH) control tests. It has accurately predicted the effect of both soil
353 amendments on soil water retention improvement in the whole tested RH range. As the soil water
354 content in the range from fully saturated to the equilibrium state under 90% RH is that covered by
355 the HYPROP-2 tests, and the curves in that range in the Fig.9 are almost same, so the RH control tests
356 are consistent with the HYPROP-2 tests. The three-phase model demonstrates the ineffectiveness
357 using the WR at relatively high soil water content range. Meanwhile it well describes the influence of
358 WR concentration on the SWRCs at low soil water content. A valuable notice from the modelling
359 results is that for the 5% WR curves of the two clayey sand soils, the water retention capacity starts
360 to decline at the high suction end (or low water content end), compared to that of the 3% WR. This
361 can be attributed to the extremely low pore water content at the situation when the WR to water



362 ratio is too high to work effectively. This can also explain that the decline of the 5% WR curve of
363 clayey sand B at high suction is much faster than that of the counterpart one of the clayey sand A. As
364 the clayey sand B has higher specific surface area, under the same water content the WR
365 concentration in the remaining soil water, particularly for the water film on pore surface, is much
366 higher than that of the clayey sand A.
367

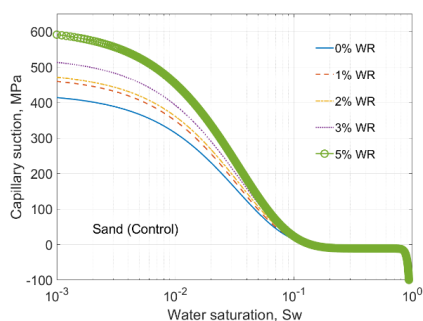


368 Fig. 9. The three-phase model modelling of the SWRCs measured by RH control tests

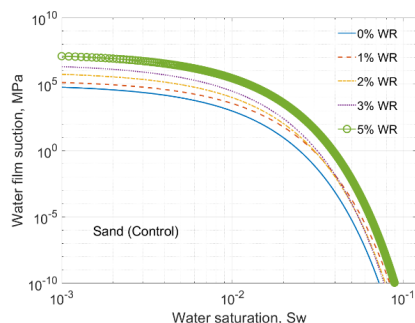
369
370 The results of three-phase model can provide further understanding of WR effect on the capillary
371 contribution (P_c) and water film contribution (P_s), respectively, in the total matric suction. Fig.10
372 shows the two components (Eqs. (5) and (8)) in the Eq. (9) for all the SWRCs. Align with what have
373 been observed in Fig. 9, it can be further seen that WR helps to enhance the P_c in high suction or low
374 soil water saturation range because WR increases the bulk water surface tension. The higher the WR
375 concentration, the higher is the increase of surface tension. The WR also enhances the P_s , particularly
376 at the low soil water saturation. Comparing with the P_c , P_s is deliberately presented in log-scale in
377 Fig. 10. The comparison illustrates that WR presents much significant effect on P_s in a form of
378 exponential trend with WR concentration. It indicates that WR is particularly active in enhancing the
379 bonding of water film with the soil particles. It can also be clearly seen that for the clayey soil A and
380 B samples, the P_s of the 5% WR decreases fast when the water saturations are about 1.1%. The
381 smaller the pore size (average pore size of clayey soil B < that of clayey soil A) the flatter the curve or
382 the less active action of the WR can be observed. Fig. 9(a), (c) and (e) show that all P_c component
383 curves converge to zero when the pore water content reaches the state of full saturation. However,



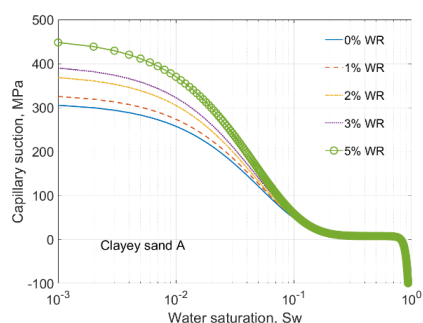
384 the P_s curves in (b), (d) and (f) intercept with the x-axis (suction = 10^{-4} Pa \approx 0) at water saturation less
 385 than 1. For the clayey sand B, there is a clear trend that the higher the WR concentration the bigger
 386 the S_w of the x-axis intercept, because clayey sand B has a high specific surface area. The higher the
 387 S_w intercept on the x-axis the less the free water in fully saturated soil samples. The modelling
 388 highlights the enhancement of the WR effect with the its concentration. Overall, the three-phase
 389 model has identified all key underlying mechanisms well and is in good agreement with what has
 390 been noticed and discussed in the experiment before.
 391



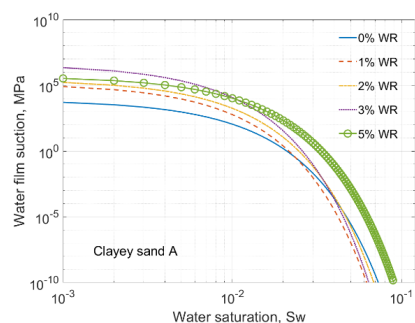
(a) Sand (Control) - P_c component



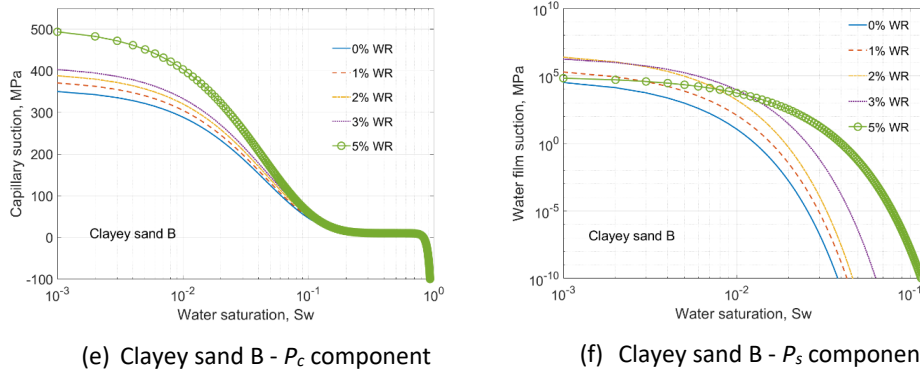
(b) Sand (Control) - P_s component



(c) Clayey sand A - P_c component



(d) Clayey sand A - P_s component



392 Fig. 10. The capillary component P_c and the water film component P_s in the three-phase modelling
 393

394 6. Characterization of the WR Concentration on the SWRCs

395 To provide guidance for effective use of the conditioning water retainer in soil water management
 396 practice, a characterization model for the WR concentration on the SWRCs is proposed. Unlike the
 397 clay amendment, which modifies the soil pore structure, the WR only modifies the interfacial forces
 398 between the three water phases in unsaturated soils but have no modification on the pore structure
 399 of soils. A WR effect model based on the three-phase SWRC model (Eq. (9)) is proposed in the form
 400 of the Eq. (10), as shown below. The added extra exponential term is to quantify the WR effect. The
 401 similar approach has been adopted for the characterization of other physical properties of
 402 unsaturated porous materials (Jin et al. 2017; Xiang et al. 2020)

403

$$404 \quad \psi_m = e^{\gamma C_{WR}} \left(\lambda \left[\frac{1}{\alpha} (\exp(\alpha S_w) - 1) - \frac{1}{\beta} (\exp(\beta(1 - S_w)) - 1) \right] + \chi(1 - S_w)^n \right) \quad (10),$$

405

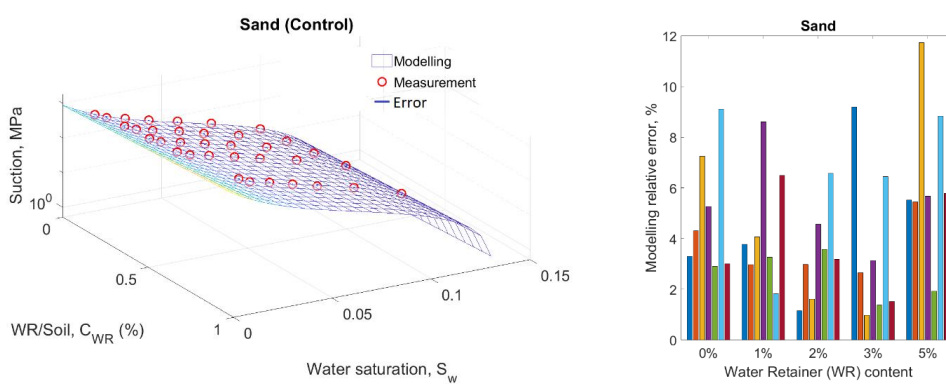
406 where γ is a constant, C_{WR} is the usage of the WR. For all the SWRC experimental tests, the WR was
 407 added in the water beforehand, then the prepared WR water solutions were mixed with oven dried
 408 soils up to saturated state. The SWRCs were measured by drying from a fully saturated state. In the
 409 drying process, the soil pore water evaporates, however, the WR is assumed not evaporable and
 410 remains in the soil. As the result, the WR concentration in soil pore water keeps increase with the
 411 drying process but the weight ratio of the WR to the soil samples remains a constant. Using the Eq.
 412 (10) to present all the SWRC measurements of a specific soil sample, we take the C_{WR} to be the initial
 413 WR to Soil weight ratio (WR/Soil) at the start of the saturated state. Fig. 11 displays the modelling
 414 results using the Eq. (10) to fit all the SWRC measurements in 3D space for the suction versus the



415 WR/Soil ratio and the soil water saturation, and the modelling relative error. It can be seen that the
416 Eq. (10) well represents the surface of suction for all the three soils. The overall modelling average
417 relative error is about 5%.

418

419

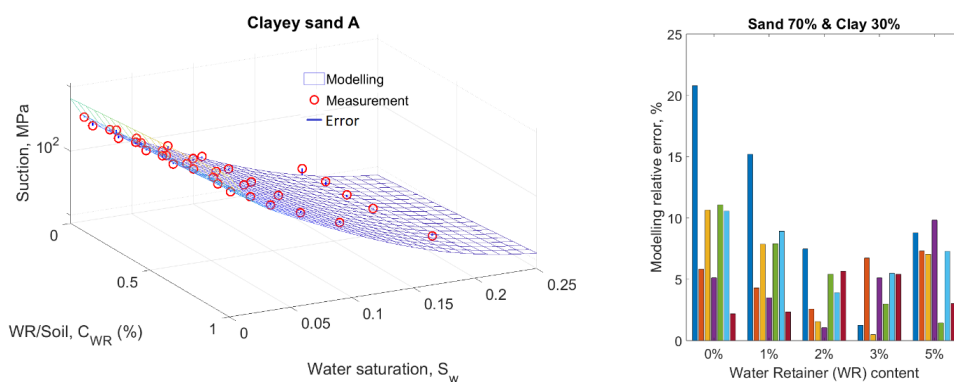


420

421

422

(a). Modelling for sand (Control)



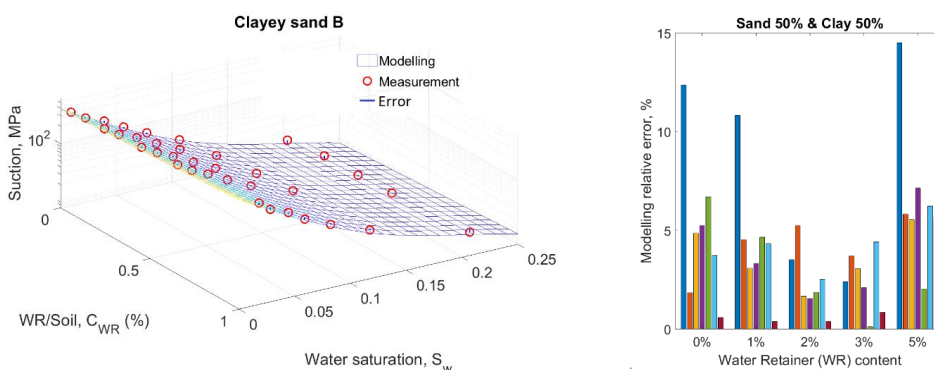
423

424

425

426

(b). Modelling for clayey sand A



427

(c). Modelling for clayey sand B

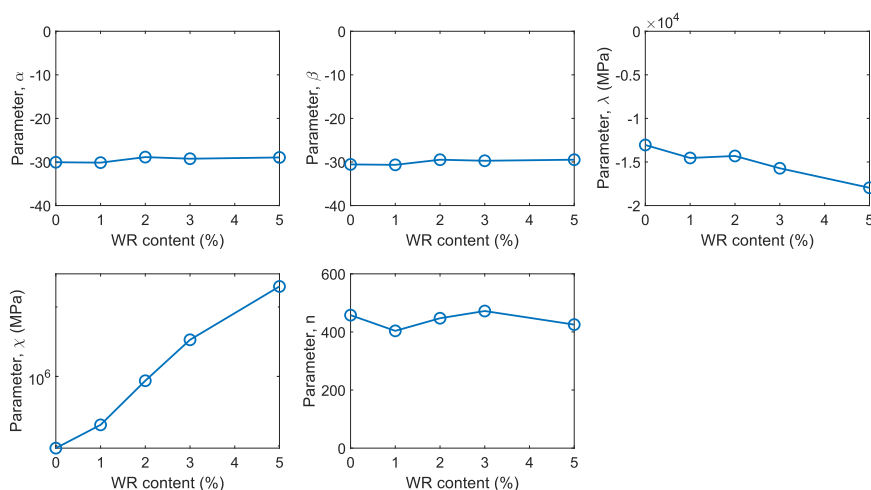
428

Fig. 11. The characterization modelling of the effect of the WR concentration on SWRCs

429

430 Fig. 12 illustrates the parametric variation of the Eq. (10) with the WR content for the three soils. It
 431 can be seen that the WR has little effect on the parameters of α and β which have a certain value for
 432 specific soils. The parameter, λ , decreases with the WR content at approximately a linear trend, while
 433 the parameter, χ , which is presented in log scale, increases exponentially until the WR at the initial
 434 saturated state reaches 3%. This is in line with previous analysis that WR particularly influences the
 435 interfacial forces between the water film and soil particles.

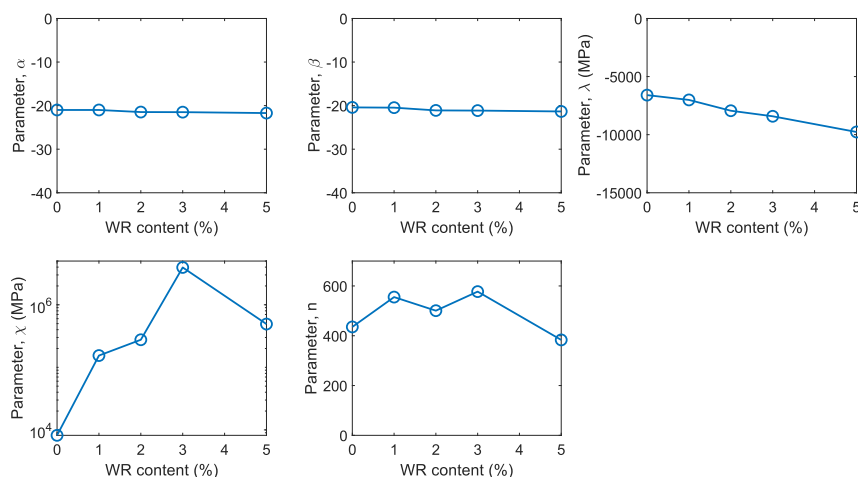
436



437

438

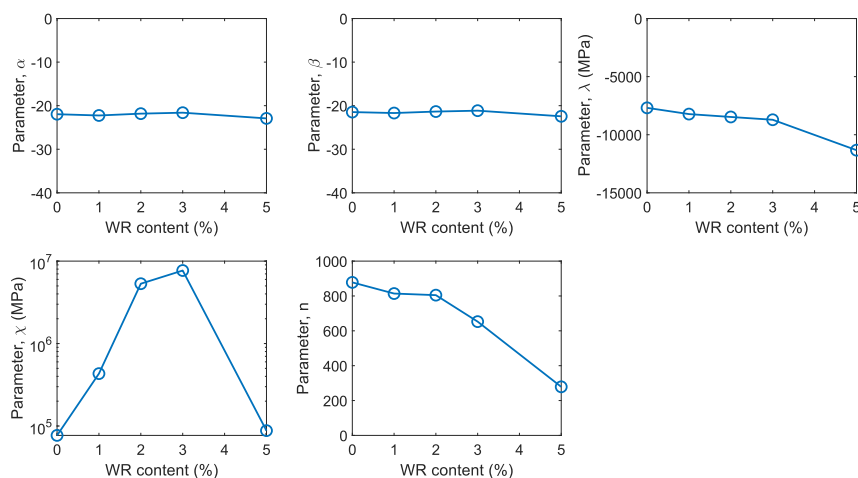
(a) Sand (Control)



439

440

(b) Clayey sand A



441

442

(c) Clayey sand B

Fig. 12. The parametric variation of the model Eq. (10) with WC content

444

445

7. Conclusions

446

447

448

449

This paper reports research on the assessment of a natural solid and a synthesised liquid soil amendments for soil water retention improvement. The soil water retention curve has been selected to comparing their effects. Two approaches were adopted to obtain a full range of the SWRCs from fully saturated to nearly dry. A new mathematical model was proposed to represent the effect the



450 amendments on SWRCs in full range of saturation and employed to characterize the WR
451 concentration effect. From the results and the analysis, the following conclusions can be drawn:

- 452 • HYPROP-2 and relative humidity control approaches together have been successfully
453 applied to assess the effect of soil amendments on soil water retention characteristic
454 curves. The measurements are stable, and the recorded curves are smooth and complete.
- 455 • Both the tested soil amendments demonstrate the effect on soil water retention
456 enhancement. The natural clay is more effective at high soil water content range while the
457 conditioning water retainer primarily works at low soil water content range. The active range
458 of 3% WR is about at the pore water saturation is less than 0.02, and 5% WR is about 0.03.
- 459 • The proposed 3-phase model demonstrates a good performance representing the SWRCs for
460 wide range of the soil water saturation from fully saturated to nearly dry. In addition, it
461 provides an advantage to assess the soil amendment agents effect on water film and bulk
462 water capillarity, respectively, which helps to well understand and interpret the working
463 mechanism of soil amendments. A derived model on it has been successfully applied to
464 quantitatively characterize the effect of the WR usages on SWRCs. The two models can be
465 useful tools for the WR application in water management practice.

466

467 **Competing interests**

468 The authors declare that they have no conflict of interest.

469

Author contribution

470 Yu Wang: conceived the concepts; funding application; proposed and conducted experiments and
471 model development; experimental and modelling results analysis, discussion and presentation; write
472 the paper.

473 Yirong Leng: performed experiments.

474 Miklas Scholz: funding application; paper editing.

475 Nora Hatvani: provided the conditioning water retainer; paper editing.

476 Vincent Uzomah: paper editing.

477

Funding

478 This work was funded by the European Union's Horizon 2020 Research and Innovation Program
479 under Grant Agreement No. 858375 (WATERAGRI project).

480

Data availability statement



481 The data presented are available on request from the corresponding author.

482

References

483 Angulo-Jaramillo, R., Bagarello, V., Prima, S.D., Gosset, A., Iovino, M., Lassabatere, L., 2019, Beerkan
484 Estimation of Soil Transfer parameters (BEST) across soils and scales. *Journal of Hydrology*. 576, 239–
485 261.

486 Beckett, C.T.S., Augarde, C.E., 2013. Prediction of soil water retention properties using pore-size
487 distribution and porosity. *Canadian Geotechnical Journal*. 50(4), 435-450.

488 Bulolo, S., Leong, E.C., Abuel-Naga, H., 2021. Filter paper method for suction measurement using
489 electrical resistivity. *Géotechnique Letters*. 11(3), 195-201.

490 Castellini, M., Prima, S.D., Moret-Fernández, D., Lassabatere, L., 2021. Rapid and accurate
491 measurement methods for determining soil hydraulic properties: A review. *J. Hydrol. Hydromech.*
492 69(2). DOI: 10.2478/johh-2021-0002.

493 Chang, C.-C. and Cheng, D.-H., 2018, Predicting the soil water retention curve from the particle size
494 distribution based on a pore space geometry containing slit-shaped spaces, *Hydrol. Earth Syst. Sci.*,
495 22, 4621–4632

496 de Lima R.P., da Silva, A.R., 2022. Soil physics: A suite of tools to fit and compare water retention
497 curves, *Soil Sci. Soc. Am. J.* 86, 658–663.

498 Dontsova, K.M., Norton, L.D., Johnston, C.T., Bigham, J.M., 2004. Influence of exchangeable cations
499 on water adsorption by soil clays. *Soil Sci. Soc. Am. J.* 68, 1218-1227.

500 Dullien, F.A.L., 1991. *Porous media fluid transport and pore structure*. USA, Academic Press Inc.

501 Edeh I.G., Mašek, O., 2022. The role of biochar particle size and hydrophobicity improving soil
502 hydraulic properties. *Eur J Soil Sci.* 73, e13138.

503 Fredlund, D.G., 1989. Soil suction monitoring for roads and airfields. *symposium state-of-the-art of*
504 *pavement response monitoring systems for roads and airfields*. West Lebanon, NH.

505 Gerrit Huibert de Rooij, 2022, Technical note: A sigmoidal soil water retention curve without
506 asymptote that is robust when dry-range data are unreliable, *Hydrol. Earth Syst. Sci.*, 26, 5849–5858



- 507 Gerrit Huibert de Rooij, Juliane Mai, and Raneem Madi, 2021, Sigmoidal water retention function
508 with improved behaviour in dry and wet soils, *Hydrol. Earth Syst. Sci.*, 25, 983–1007.
- 509 Hall, C., Hoff, W.D., 2002, *Water Transport in Concrete and Masonry Materials*, Published by Taylor
510 & Francis Group, London and NY.
- 511 Huang, W., Lai, H., Du, J., Zhou, C., Liu, Z., Ni, Q., 2022. Effect of polymer water retaining agent on
512 physical properties of silty clay. *Chem. Biol. Technol. Agric.* 9, 47.
- 513 Iwamatsu, M., Horii, K., 1996. Capillary condensation and adhesion of two wetting surfaces. *Journal*
514 *of Colloid and Interface Science.* 182, 400-406.
- 515 Jin, H., Wang, Y., Zheng, Q., Liu H., Chadwick, E., 2017. Experimental study and modelling of the
516 thermal conductivity of sandy soils of different porosities and water contents, *Applied Sciences.* 7,
517 119.
- 518 Jin, H., Wang, Y., Zheng, Q., Liu, H. and Chadwick, E., 2017, Experimental Study and Modelling of the
519 Thermal Conductivity of Sandy Soils of Different Porosities and Water Contents, *Applied Sciences* 7:
520 119
- 521 Keiblinger, K.M., Kral, R.M., 2018. Sustainable intensification of agricultural production: A review of
522 four soil amendments. *Bodenkultur.* 69, 141–153.
- 523 Lassabatere, L., Angulo-Jaramillo, R., Ugalde, J.M.S., Cuenca, R., Braud, I., Haverkamp, R., 2006.
524 Beerkan estimation of soil transfer parameters through infiltration experiments—BEST, *Soil Sci. Soc.*
525 *Am. J.* 70, 521–532.
- 526 Lebeau, M., Konrad J.M., 2010. A new capillary and thin film flow model for predicting the hydraulic
527 conductivity of the unsaturated porous media. *Water Resources Research.* 46, W12554.
- 528 Lemos, L.T.O., de Deus, F.P., Thebaldi, M.S., Diotto, A.V., de Andrade Júnior, V.C., de Almeida, R.C.,
529 2021. Influence of the soil water retention curve type and magnetic water treatment on lettuce
530 irrigation management responses. *Water Supply.* 21, 2850–2862.
- 531 Likos, W.J., 2009. Pore scale model for water retention in unsaturated sand, The 6th international
532 conference on micromechanics of granular media, *API Conference Proceeding.* 1145.



- 533 Likos, W.L., Ning Lu, N., 2002. Filter paper technique for measuring total soil suction. Transportation
534 Research Record: Journal of the Transportation Research Board. 1786(1), 120-128.
- 535 Meter Group, [https://www.metergroup.com/en/meter-environment/products/hyprop-2-soil-
moisture-release-curves](https://www.metergroup.com/en/meter-environment/products/hyprop-2-soil-
536 moisture-release-curves)
- 537 Miller, J.J., Beasley, B.W., Drury, C.F., Larney, F.J., Hao, X., Chanasyk, D.S., 2018. Influence of long-
538 term feedlot manure amendments on soil hydraulic conductivity, water-stable aggregates, and soil
539 thermal properties during the growing season. Canadian Journal of Soil Science. 98(3), 421-435.
- 540 Mohammadi, M.H., Meskini-Vishkaee, F., 2012. Predicting the film and lens water volume between
541 soil particles using particle size distribution. Journal of Hydrology. 475, 403-414.
- 542 Mohawesh, O., Durner, W., 2019. Effects of bentonite, hydrogel and biochar amendments on soil
543 hydraulic properties from saturation to oven dryness. Pedosphere. 29, 598–607.
- 544 Mualem, Y., 1989, Modelling the Hydraulic Conductivity of Unsaturated Porous Media, in Indirect
545 Methods for Estimating the Hydraulic Properties of Unsaturated Soils, M. Th. van Genuchten and F.
546 J. Leij (ed.), Proceedings of the International Workshop on Indirect Methods for Estimating the
547 Hydraulic Properties of Unsaturated Soils Riverside, California, October 11-13.
- 548 Murray, H.H., 2000. Traditional and new applications for kaolin, smectite, and palygorskite: A general
549 overview. Appl. Clay Sci. 17, 207–221.
- 550 Or, D., Tuller, M., 1999. Liquid retention and interfacial area in variably saturated porous media:
551 Upscaling from single-pore to sample-scale model. Water Resources Research. 35(12), 3591-3605.
- 552 Orzeszyna, H., Garlikowski, D., Pawlowski, A., 2006. Using of geocomposite with superabsorbent
553 synthetic polymers as water retention element in vegetative layers. Int. Agrophys. 20, 201–206.
- 554 Rahmati, M., Vanderborght, J., Šimůnek, J., Vrugt, J.A., Moret-Fernández, D., Latorre, B., Lassabatere,
555 L., Vereecken, H., 2020, Soil hydraulic properties estimation from one-dimensional infiltration
556 experiments using characteristic time concept. Vadose Zone J. 19, e20068.
- 557 Salas-García, J., Garfias, J., Martel R., Bibiano-Cruz, L., 2017. A low-cost automated test column to
558 estimate soil hydraulic characteristics in unsaturated porous media. Geofluids. 6942736.



- 559 Spitalniak, M., Bogacz, A., Zieba, Z., 2021. The assessment of water retention efficiency of different
560 soil amendments in comparison to water absorbing geocomposite. *Materials*. 14, 6658.
- 561 Spitalniak, M., Lejcus, K., Dabrowska, J., Garlikowski, D., Bogacz, A., 2019. The influence of a water
562 absorbing geocomposite on soil water retention and soil matric potential. *Water*. 11, 1731.
- 563 Tokunaga, T.K., 2011. Physicochemical controls on adsorbed water film thickness in unsaturated
564 geological media. *Water Resources Research*. 74, W08514.
- 565 Tuller, M., Or, D., Dudley L.M.,. 1999. Adsorption and capillary condensation in porous media:
566 Liquid retention and interfacial configurations in angular pores. *Water Resources Research*. 35(5):
567 1949-1964.
- 568 Wang, S., Zhao, X., Zhang, J., Jiang, T., Wang, S., Zhao J., Meng, Z., 2023. Water retention
569 characteristics and vegetation growth of biopolymer-treated silt soils. *Soil & Tillage Research*. 225,
570 105544.
- 571 Wang, Y., Grove, S.M., Anderson, M.G., 2008. A physical-chemical model for the static water
572 retention characteristic of unsaturated porous media. *Advances in Water Resources*. 31, 723-735.
- 573 Wang, Y., Grove, S.M., Anderson, M.G., 2008. A physical–chemical model for the static water
574 retention characteristic of unsaturated porous media. *Advances in Water Resources*. 31(4), 701-713.
- 575 Wang, Y., Hu, L., Luo, S., Lu, N., 2022. Soil water isotherm model for particle surface sorption and
576 interlamellar sorption, *Vadose Zone J*. 21, e20221.
- 577 Wang, Y., Ma, R., Zhu, G., 2022. Improved prediction of hydraulic conductivity with a soil water
578 retention curve that accounts for both capillary and adsorption forces. *Water Resources Research*.
579 58, e2021WR031297.
- 580 Wang, Y., Wang X-Y., Scholz, M., Ross, D.K., 2012, A physico-chemical model for the water vapour
581 sorption isotherm of hardened cementitious materials. *Construction and Building Materials*. 35, 941–
582 946.
- 583 Wanniarachchi, D., Cheema, M., Thomas, R., Kavanagh, V., Galagedara, L., 2019. Impact of soil
584 amendments on the hydraulic conductivity of boreal agricultural podzols. *Agriculture*. 9, 133.



- 585 Xerdiman, D., Zhou, H., Li, S., Sun, H., Xin, K., Sun, D., Li, C., 2022. Effects of water-retaining agent
586 dosages on slope-protection plants and soil nutrients on rocky slopes. *Sustainability*. 14, 3615.
- 587 Xiang, N., Wang, Y., Oleiwi, H., Chadwick, E., Augusthus-Nelson, L., Chen, X., Shabalin, I., 2020,
588 Modelling Concrete Electrical Resistivity at Varied Water, Chloride Contents and Porosity, *Magazine*
589 *of Concrete Research*, 72(11): 552–563
- 590 Zhang, C., Lu, N., 2020. Soil sorptive potential: its determination and predicting soil water density. *J.*
591 *Geotech. Geoenviron. Eng.* 146, 04019118.
- 592 Zhou, H., Chen C., Wang, D., Arthur E., Zhnag, Z., Guo, Z., Peng, X., Mooney, S.J., 2020. Effect of
593 long-term organic amendments on the full-range soil water retention characteristics of a Vertisol.
594 *Soil & Tillage Research*. 202, 104663.